Separation and Purification Technology 362 (2025) 131525

Contents lists available at ScienceDirect

Separation and Purification Technology

journal homepage: www.elsevier.com/locate/seppur

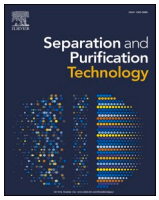

Extractive separations of lithium isotopes with benzo-15-crown-5 and ionic liquids: A comparative study between stirred vessels and small channel contactors

Cong Duan [a], Shijia Sun [b], Haoyu Wang [a], Mohd Tarique [c,d], Edward Tipper [c], Tamsin Whitfield [e,f], Mark R. Gilbert [e], Panagiota Angeli [a,*]

[a] ThAMeS Multiphase, Department of Chemical Engineering, UCL, UK
[b] Department of Chemistry, UCL, UK
[c] Department of Earth Sciences, University of Cambridge, UK
[d] National Centre for Polar and Ocean Research, Ministry of Earth Sciences, Goa, India
[e] United Kingdom Atomic Energy Authority, Culham Campus, Abingdon, Oxon, UK
[f] Department of Materials, University of Oxford, UK

ARTICLE INFO

Editor: Raquel Aires Barros

Keywords:
Liquid-liquid extraction
Lithium isotopes separation
Process intensification
Small channel contactors
Ionic liquids
Benzo-15-crown-5

ABSTRACT

The separation of lithium and the fractionation of the isotopes by solvent extraction was studied, using benzo-15-crown-5 as an extractant dissolved in a diluent of an ionic liquid and anisole. Particularly, the continuous extractive fractionation of the lithium isotopes was investigated in small channels for the first time. Depending on the composition of the diluent, 4–25 % of the lithium was extracted in stirred vessels with a fractionation factor of 1.026 (±0.002) over an hour. In comparison, in the small channel contactors with 0.5 mm diameter, about 8–19 % extraction was reached in approximately 1 min with an apparent fractionation factor of 1.032 (±0.005). An increase in residence time in the channels increased the extraction percentage but reduced the degree of lithium fractionation. When the ionic liquids were diluted with anisole, equilibrium was reached faster while the extraction percentage was not affected in stirred vessels. Density Functional Theory (DFT) calculations suggested that the fractionation of the Li isotopes is attributed to different vibrational frequencies of the Li-O bonds with the extractant in the organic solution and with water. The results also revealed that the ionic liquid facilitates the isotope fractionation, while dilution of the ionic liquid with anisole did not affect fractionation.

1. Introduction

In natural resources, lithium isotopes can be significantly fractioned by secondary mineral formation and/or adsorption onto particles [1]. Lithium isotopes are important in many applications including nuclear fusion reactions, fusion power plants, and for tracing continental weathering processes [2–4]. Producing lithium with isotopic concentrations enriched beyond natural levels is essential in many technological fields. For example, most contemporary fusion reactors use deuterium and tritium as the fuel. Tritium is a radioactive gaseous substance, and its small atomic size allows it to permeate through materials easily, making its containment and capture difficult. It must be generated in situ inside the reactor using lithium-based materials in breeding blankets. For future fusion power plants to be self-sufficient in tritium, large amounts of lithium enriched to at least 10 % lithium-6 will be required in most design scenarios [5]. In some other applications, such as in pressurized water reactors (PWRs), lithium hydroxide is added as a coolant to stabilize pH levels and reduce corrosion in the primary water systems. The existence of lithium-6 could create an environment where significant quantities of tritium is produced. Thus, lithium in this case must be enriched to at least 99.995 % of lithium-7 to be used in PWRs, as recommended by the Oak Ridge National Laboratory [6].

The enrichment of lithium isotopes to date has predominantly been via the COLEX process which involves the fractionation of the Li isotopes from an acidic solution into a mercury amalgam. This method separates

* Corresponding author.
E-mail address: p.angeli@ucl.ac.uk (P. Angeli).

https://doi.org/10.1016/j.seppur.2025.131525
Received 7 November 2024; Received in revised form 7 January 2025; Accepted 8 January 2025
Available online 10 January 2025

lithium-6 and lithium-7 based on their different affinity to mercury, and it is attractive due to the large and compelling single-stage separation factor of $\alpha = 1.054$ ($\pm$ 0.002) [7] (also referred to as fractionation factor, the molar ratio of the heavier to the lighter isotope between the two phases). There are, however, significant environmental concerns with the COLEX process because of the mercury vapour emissions [8]. There is a growing need to develop sustainable, economic, and more environmentally friendly lithium isotope separation methods. Alternative techniques such as chromatography [9], electromigration [10], membrane separation [11], and use of lasers [12] have been considered. Extractive separations are one of the promising alternative methods which involve fractionation during extraction from aqueous solutions to organic diluents using suitable extractants [13,14]. Extractive separations can benefit from many advantages such as low energy consumption and selectivity.

There are two general aspects to be considered for lithium extractive separations: chemical systems and separation units. Considerable research has been directed towards optimising the chemical systems for the extraction, all in stirred vessels or batch reactors. For example, with respect to the extractant, cryptands with suitable sized cavities to accommodate the lithium ion (such as 2. 1. 1-cryptand) can be used for lithium fractionation [15,16]. Crown ether extractants can be made more hydrophobic by adding a lipophilic group to the carbon atoms, thus reducing the amount of extractant lost to water through dissolution [17,18]. The crown ether benzo-15-crown-5 (B15C5) has demonstrated both high fractionation factors (around 1.040 $\pm$ 0.003) and moderate distribution factors (defined as the ratio of lithium in the organic phase to the aqueous phase), and is also suitable for industrial applications due to its low cost [19], indicating efficient fractionation and extraction for lithium [20–26]. As a greener option compared to organic solvents, ionic liquids (ILs) can be used as diluents for extractions [27]. For example, imidazolium-based ionic liquids have been widely used as diluents in the recycling and separation of metal ions, such as Li(I), Pb(II), Au(III), Pt (IV), Pd(II), Sr(II), U(VI), and other rare-earth elements in liquid–liquid adsorption/extraction and membrane systems [23,24,28,29]. In recent studies, a combination of crown ether, ionic liquids, and organic solvents for dilution has been proposed as an effective and sustainable approach for lithium extraction separations [18,30,31]. A few studies also investigated the factors affecting lithium isotope extractions using ionic liquids, including solvent composition, effect of solvent dilution, extractant/lithium concentration, temperature, and pH [32,33].

In most cases, only equilibrium studies of the chemical systems discussed above have been carried out. Such studies take place in stirred vessels and have typically long residence times of a few hours; as a result they provide little information on the kinetics of the extraction, which can be important in a system where overall separation and isotopic fractionation are occurring at similar times. Small channel contactors provide a more conducive platform for detailed kinetic studies compared to stirred vessels. They have been shown to intensify liquid–liquid extractions because of large specific interfacial areas which enhance mass transfer, controllable and reduced residence times, well-defined flow patterns, and simplified modelling [34,35]. There are many studies highlighting the promising aspects of using small channel devices for process intensification. For example, Pheasey et al. found that 80 % extraction efficiency of Nd was achieved in a 0.5 mm channel in 37.5 s, while similar extraction percentage needed about 16 h in batch separators [36]. Intensified extractions in short times of metal ions, such as uranium[37], lanthanum [38], europium [39], and selective separation of Co/Ni [40], have already been demonstrated. However, there are no reports for the application of lithium fractionation in small channel contactors.

Previous studies considered the development of suitable chemistries for the sustainable fractionation of lithium with solvent extraction in equilibrium conditions, which were, thus, carried out in batch vessels. In this work, for the first time, we investigate small channel flow contactors to intensify the continuous process of lithium isotope fractionation. In addition, we thoroughly investigate the mechanism of lithium extraction and isotope fractionation via Density Functional Theroy (DFT) calculations to account for the alternative reaction pathways and to better understand the effects of solvation environment. The composition of the organic phase is particularly important in flow systems, where the phase properties affect the flow patterns and influence the mass transfer. The crown ether B15C5 is used as an extractant to separate lithium isotopes originally existing in aqueous solutions. An ionic liquid (1-butyl-3-methylimidazolium bis(trifluoromethylsulfonyl)imide) is chosen as a diluent. The ionic liquid is, however, more expensive and viscous compared to traditional solvents. Thus, the effect of diluting the ionic liquid with methoxybenzene (anisole, $CH_3OC_6H_5$) is also studied. The composition of the chemicals forming the two phases has been based on previous research at equilibrium conditions to ensure optimal lithium separation and applicability [23,29]. The lithium extraction and isotope fractionation are studied both in stirred vessels and in small channel contactors, and the results are compared in terms of residence time, extraction percentage, and fractionation factor. The enhanced lithium separation is explained in terms of vibrational frequencies of the bonds of the possible complexes formed during extraction and of thermodynamic parameters via DFT calculations, while the role of ionic liquid and of the added anisole are also discussed.

2. Materials, experimental procedure, and models

2.1. Materials

Lithium chloride (CAS number: 7447-41-8, purified >98 %) was purchased from VWR Chemicals; ionic liquid (cation: 1-butyl-3-methylimidazolium, abbreviated as $[C4mim]^+$ below; anion: bis(trifluoromethylsulfonyl)imide, abbreviated as $[NTf2]^-$ below) (CAS number:174899-83-3, >98 %), benzo-15-crown-5 (B15C5) (CAS number: 14098-44-3, >98 %), and anisole (CAS number: 100-66-3, >99 %) were purchased from Sigma Aldrich; all chemicals were used as received. The aqueous phase consists of lithium chloride dissolved in deionized water. The organic phase is either pure ionic liquid (IL) or ionic liquid diluted with anisole (volume ratio IL: anisole = 3:7) and the added extractant B15C5. The two liquid phases were prepared at room temperature. Each phase is contacted and pre-saturated with the other phase before lithium salt is added to the aqueous phase. The physical properties of the fluids used in the experiments have been measured in the lab and are listed in Table 1. Viscosity was measured with a Rheometer DV-111 Ultra (Brookfield), with an error of 1 %, and surface and interfacial tensions were measured with a DSA100E tensiometer (KRÜSS Scientific), with an error of $\pm$0.3 mN/m. The results for the physical properties agree well with measurements done for similar chemical mixtures [41,42].

2.2. Experimental methodology

The extraction experiments were carried out at atmospheric pressure and room temperature (T = 293 K). Equilibrium experiments were carried out first in stirred vessels. For these experiments, equal volumes of the aqueous and the organic phase solutions (5 mL) were added in stoppered vessels and then mixed with a magnetic stirrer at constant rotational speed of 800 rpm for up to 1 h. A sample from the aqueous phase was removed from the vessel every 10 mins for the concentration measurements. The same amount of the organic phase was also removed from the vessel to keep the volumes of the two phases equal at all times. Prior studies on lithium separation have indicated that the composition of the organic phase influences the extraction percentage [43]. Here we have considered two solvent compositions in the organic phase, either ionic liquid on its own or a mixture of ionic liquid and anisole at a 3:7 vol ratio. The 3:7 vol ratio is chosen to achieve maximum in extraction percentage as reported by Liu et al. [29]. The concentration of lithium chloride in the aqueous phase is constant at 0.5 mol/L for all the cases

Table 1
Physical properties of the fluids used in experiments measured at room temperature (293 K) and ambient pressure.

Fluids	Extractantconcentration /mol/L	Density /kg•m^{-3}	Viscosity /cP	Interfacial tension with aqueous solution /mN•m^{-1}
LiCl aqueous solution	n/a	1007± 2	1.002± 0.01	n/a
Pure ionic liquid [C4mim][NTf2]	0.2	1415± 2	56.364± 0.6	12.33± 0.3
	0.4	1395± 2	62.071± 0.6	12.25± 0.3
	0.5	1392± 2	65.689± 0.7	12.15± 0.3
IL/Anisole (volume ratio: 3/7)	0.2	1101± 2	3.012± 0.03	54.11± 0.3
	0.4	1105± 2	3.250± 0.03	53.24± 0.3
	0.5	1113± 2	3.435± 0.03	53.40± 0.3

studied, and the extractant concentrations are from 0.1 to 0.5 mol/L in the organic phase. Six cases named from A to F are further considered, and the composition of the organic phase for these cases is listed in Table 2.

Fig. 1 shows the experimental set-up for the continuous small channel extraction. The aqueous and organic phases were injected separately by two high precision continuous syringe pumps (Kd Scientific) via polytetrafluoroethylene (PTFE) tubes that had the same diameter (d = 0.5 mm) and joined in a T-junction mixer made of fluorinated ethylene propylene (FEP). The mixture of the two phases was introduced to the small channel contactor made of PTFE. The organic phase was the continuous one and entered in line with the main channel, while the aqueous solution containing the lithium salt was fed from the orthogonal direction. A high-speed camera (Phantom v1212) is utilised to analyse the flow patterns of the two-phase flow. Illumination is provided by an LED panel located on the opposing side. To enhance the imaging quality, a visualisation box containing a water-glycerol mixture with a matched refractive index to that of the PTFE tubing is employed to enclose the tubing. At the end of the extraction channel the mixture of the two phases was collected in a narrow glass container and shortly after samples from both phases were taken with a pipette for analysis.

The lithium concentrations in the aqueous solutions before and after the extraction were measured using Agilent MP-AES in the Department of Chemical Engineering at UCL. The uncertainty of the measurements was 6.07 %. Lithium isotope ratios were measured on a Neptune multi-collector ICP-MS using an APEX IR sample introduction system, and 50micl/min PFA nebuliser nickel X cones. ^{7}Li/^{6}Li ratios were normalised to L-SVEC (NIST RM 8545) using standard-sample bracketing and reported using standard delta notation:

$$\delta^{7}Li_{x} = \left[\left(\frac{(^{7}Li/^{6}Li)_{sample}}{(^{7}Li/^{6}Li)_{standard}}\right) - 1\right]10^{3} \quad (1)$$

Therefore, $\delta^{7}Li$ shows how much the composition of the sample deviates from that of the standard. Bracketing measurements are taken for both the standard and the actual samples. The bracketing measurement sequence is designed to minimize the influence of any drift in the instrument beam strength. Since the solutions contained pure Li, no ion-chromatography separations were conducted to further purify them. Solutions were diluted to ~0.5 ppb using 10^{13} Ω resistors on the pre-amplifiers for both ^{6}Li and ^{7}Li. The typical beam size for samples was around 0.3 V on ^{7}Li and the background was typically <0.25 mV. Accuracy and precision were monitored using ^{6}Li-N and ^{7}Li-N solutions which gave values of −8.1 ± 0.6 ‰ (2SD, n = 59) and 30.3 ± 0.9 ‰ (2SD, n = 50) respectively during the course of the measurements [44,45]. These values agree with previously published values for these standards (^{7}Li-N = 30.2 ‰ and ^{6}Li-N = −8.0 ‰ to −8.3 ‰).

Table 2
Composition of the organic phase.

Cases	B15C5 Extractant concentration (mol/L)	Organic phase composition
A	0.2	IL/Anisole (volume ratio: 3:7)
B	0.4	
C	0.5	
D	0.2	Pure IL
E	0.4	
F	0.5	

2.3. Lithium separation calculations

To characterise the overall amount of lithium (including both ^{6}Li and ^{7}Li) extracted into the organic phase, the extraction efficiency (as a percentage), E, and the distribution coefficient, D, were used which are defined as follows:

$$E = \frac{n_{org}}{n_{aq,0}} = \frac{C_{org}V_{org}}{C_{aq,0}V_{aq,0}} = \frac{C_{aq,0}V_{aq,0} - C_{aq,eq}V_{aq,eq}}{C_{aq,0}V_{aq,0}} \times 100\% \quad (2)$$

and

$$D = \frac{C_{org,0}}{C_{aq,eq}} = \frac{C_{aq,0} - C_{aq,eq}}{C_{aq,eq}} \quad (3)$$

where n, C, V denote the molar amount of lithium, concentration of lithium ion in solution, and volume of the solution used in the experiment, respectively. The subscripts *aq* and *org* denote the aqueous phase and the organic phase, while *eq* and 0 represent equilibrium and initial conditions, respectively. As for the fractionation of lithium isotopes during extraction, mass balance was used to determine delta ^{7}Li in the organic phase, with $\delta^{7}Li$ measured in the aqueous phase:

$$\delta^{7}Li_{org} = \frac{\delta^{7}Li_{aq,0} - N_{aq}{}^{*}\delta^{7}Li_{aq}}{N_{org}} \quad (4)$$

where N stands for the molar fraction of lithium substance remaining in each phase over the overall lithium initially present in the aqueous solution. This can be used to determine the fractionation factor α defined as follows:

$$\alpha_{x1-x2} = \frac{(^{7}Li/^{6}Li)_{x1}}{(^{7}Li/^{6}Li)_{x2}} \quad (5)$$

where $\left(^{7}Li/^{6}Li\right)_{x}$ represents the molar ratio of Li-7 to Li-6 in phase x. In this work, x1 stands for the aqueous phase, and x2 denotes the organic phase. For cases where the fractionation factor α is close to unity (which is typical of many isotope separation techniques in one stage), the following equation can be used as a close approximation to calculate the fractionation factor α [46]:

$$\delta^{7}Li_{aq-org} = \delta^{7}Li_{aq} - \delta^{7}Li_{org} \cong 1000\left(\alpha_{aq-org} - 1\right) \cong 1000\ln\left(\alpha_{aq-org}\right) \quad (6)$$

where the $(aq-org)$ represents the two phases between which the fractionation takes place. If $\delta^{7}Li_{aq}$ is positive and therefore $\delta^{7}Li_{org}$ is negative, it indicates that there is an enrichment of lithium-6 in the

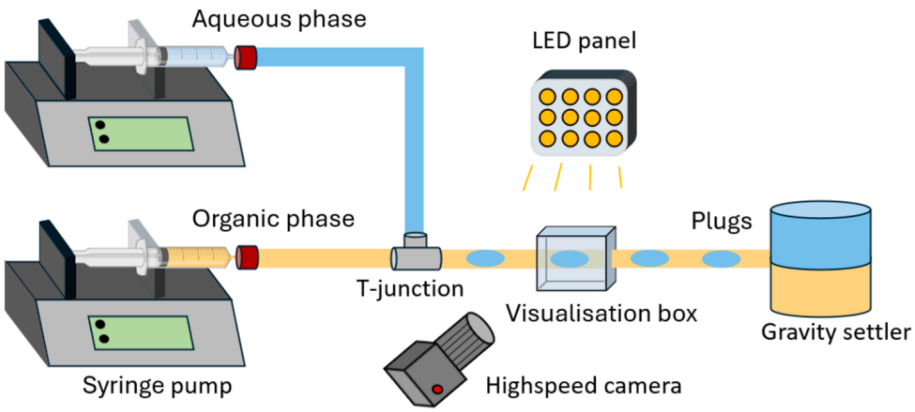

Fig. 1. Experimental setup for the continuous flow experiments in small channel contactors.

organic phase and accordingly a depletion of lithium-6 in the aqueous phase ($(\alpha_{aq-org}) > 1$).

3. Results and discussion

3.1. Equilibrium studies in stirred vessels

In the equilibrium experiments in stirred vessels, concentrations were measured every 10 min from the start of the experiment and for 1 h, and the results are shown in Fig. 2. Solid points denote anisole-diluted IL as the diluent phase, and hollow points stand for pure IL diluent. First, the effect of extractant concentration is studied. In Fig. 2 (a), the extraction percentages monotonically increase with the extractant concentration for both diluents. Slightly different extraction percentages for the two compositions were found; more importantly, the error bars for pure ionic liquids in Fig. 2 (a) are significantly larger than those of the anisole mixture. Thus, the extraction percentages for six cases are considered to investigate further the change of extraction percentage over time, and the results are plotted in Fig. 2 (b). As it can be seen Fig. 2 (b), equilibrium was established at an early stage for all the anisole-diluted cases and no significant changes of extraction percentage were found over time. However, for the pure IL cases, the extraction percentage shows a delay before equilibrium is reached regardless of extractant concentration. The final values of extraction percentage were mainly influenced by the extractant concentration. Larger concentration of extractant gives larger extraction percentage at equilibrium, which confirms the key role of B15C5 in separating lithium from aqueous solutions. The addition of anisole in the ionic liquid diluent does not affect the final extraction percentage apart from the case of 0.4 mol/L extractant, where it decreases slightly. It seems that the addition of anisole in the ionic liquid shortens the extraction time (by reducing the time to equilibrium) without impacting the final extraction percentage compared to pure ionic liquid. Diluting the IL is favourable in industrial applications for both saving ionic liquid and relaxing the pump requirements of the diluent.

Some studies have considered the role of organic diluent in lithium transfer. For example, Zhang et al. added lithium salts into aqueous solutions of B15C5 and found that only trace amounts of lithium were captured by B15C5 in water [33]. Their findings suggested that B15C5 is less able to combine with lithium ions in aqueous solvation environments. Their experiments could help explain why diluting ionic liquids with anisole increases the rate at which equilibrium is reached. The solvation power of a solvent can be expressed by polarity and can be measured by permittivity (dielectric constant). The permittivity of [C4mim][NTf2] and anisole is 12.7 and 4.3 ($C^2{\cdot}(N{\cdot}m^2)^{-1}$) respectively, while water has a high permittivity of 80.2 ($C^2{\cdot}(N{\cdot}m^2)^{-1}$) at 20 °C [33,47]. When lithium chloride is dissolved in water, its corresponding cation, lithium, does not exist on its own. Instead, a tetrahedral-shaped complex with a lithium ion in the centre surrounded by four water molecules is the optimised form in the aqueous environment. The tetrahedral-shaped complex ($[Li(H_2O)_4]^+$) has strong steric hindrances, preventing the combination of lithium with B15C5 outside the complex. With the addition of anisole, the permittivity of the organic mixture decreases from 12.7 (pure ionic liquid) to around 6.8 ($C^2{\cdot}(N{\cdot}m^2)^{-1}$). It is

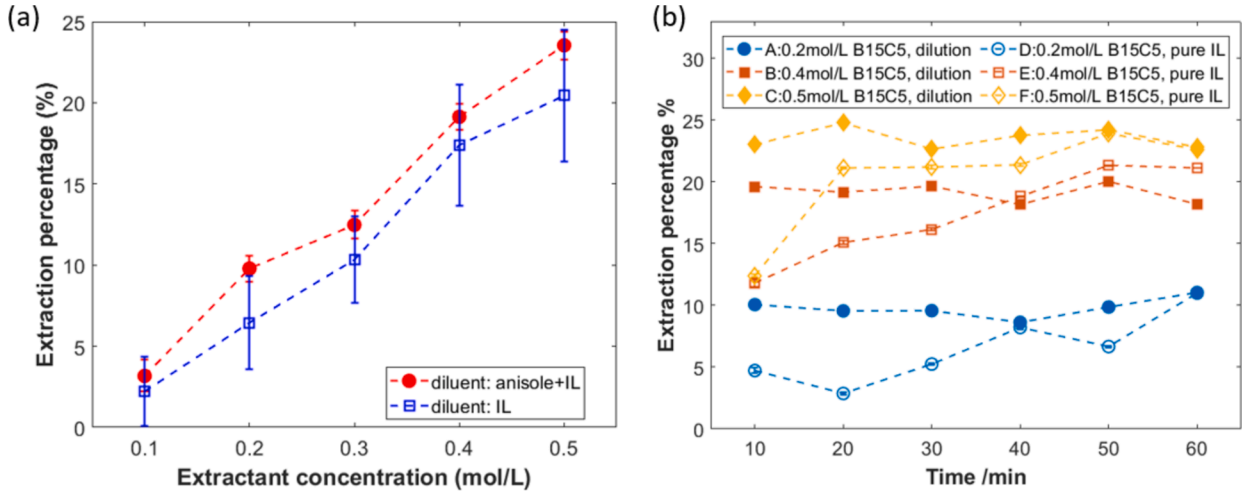

Fig. 2. (a) Extraction percentage in the equilibrium experiments varies over extractant concentration; (b) Extraction percentage at different extraction times for cases A-F. In some cases, the size of the error bar is smaller than the size of the symbol.

possible that when the $[Li(H_2O)_4]^+$ complex approaches the water-solvent interface, the IL-anisole mixture repels the H_2O molecules of the complex to the water side. This helps to reduce steric hindrances and exposes the lithium ions to the extractant, facilitating its faster transfer to the organic phase.

Some studies have suggested that the extraction is facilitated by forming complexes of lithium-ions and crown ethers through the ion–dipole interactions. The positively charged [n (crown ether) – Li]$^+$ complex is paired with bis(trifluoromethanesulfonate) ([NTf_2]$^-$) anions following the Hofmeister series [17]. Assuming a similar mechanism in the extractions here, the reaction formulation for lithium extraction when equilibrium is reached can be written as:

$$\begin{aligned} &LiCl(aq) + \{[C_4mim][NTf_2]\}(org) + n[B15C5](org) \\ \Leftrightarrow &\{[Li - n(B15C5)][NTf_2]\}(org) + \{[C_4mim]Cl\}(aq) \end{aligned} \tag{7}$$

where the *aq* and *org* in brackets are used to indicate the phase where the complexes are in. The box brackets are used for either ion pair under ion–dipole interaction or ions with long formulas when necessary, and the brace brackets are used for ion pairs under electrostatic interaction. The equilibrium constant K, and the distribution coefficient D are defined as

$$K = \frac{\{[Li - n(B15C5)][NTf_2]\}\{[C_4mim]Cl\}}{[LiCl]\{[C_4mim][NTf_2]\}[B15C5]^n} \tag{8}$$

and

$$D = \frac{\{[Li - n(B15C5)][NTf_2]\}}{[LiCl]} \tag{9}$$

Arranging the equations for K and D gives

$$K = D \times \frac{\{[C_4mim]Cl\}}{\{[C_4mim][NTf_2]\}[B15C5]^n} \tag{10}$$

The following equation can then be used to predict the number of crown ethers n that are engaged in caging a lithium ion:

$$\begin{aligned} \mathrm{Log}D &= n \times \log[B15C5] + \log\{[C_4mim][NTf_2]\} + \mathrm{logK} - \log\{[C_4mim]Cl\} \\ &= n \times \log[B15C5] + constant \end{aligned} \tag{11}$$

The logarithms of the distribution coefficient and the extractant concentration are plotted in Fig. 3, where only equilibrium concentrations after 30 min were used for the calculation of D. The number of crown ethers is found to be 1.24 for the anisole-diluted cases (D_1) and slightly larger (1.29) for the pure IL cases (D_2), indicating that there might be a hybrid complex of [n (crown ether) – Li]$^+$ with both n = 1 and n = 2 at a certain proportion, while the one-to-one complex [(crown ether) – Li]$^+$ dominates. Considering that the extraction percentage never exceeds 25 % and ignoring the loss of extractants into water, there could still be unoccupied extractants after 1 h of extraction for all cases. With the results in Fig. 3, the addition of anisole into IL slightly increases the utilisation of crown ethers by reducing the formation of [2 (crown ether) – Li]$^+$. This aligns with the conclusion that the addition of anisole does not influence the equilibrium significantly. The effect of anisole on equilibrium is also further investigated by the DFT calculations in section 3.2.

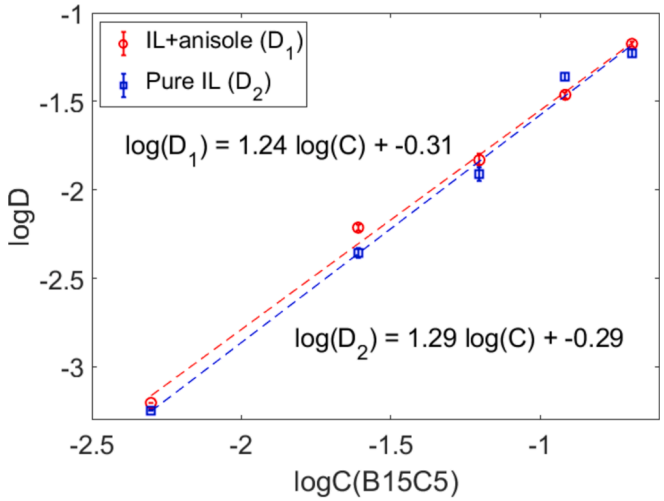

Fig. 3. Linear regression of log$D$ with log$C$(B15C5). D_1 : diluted IL solution, volume ratio = 7 anisole: 3 IL; D_2 : pure IL.

To obtain the fractionation of lithium isotopes, samples from the aqueous solutions before and after extraction were ionized and measured. The relative amounts of the two lithium isotopes were given in delta notation defined in Eq. (1). It was found that all the measured δ^7Li values are greater than those of the initial solution, indicating that lithium-7 is enriched in the aqueous phase during the extraction while lithium-6 is enriched in the organic phase. Combining Eqs. (5) and (6) and rearranging gives

$$\delta^7 Li_{org,eq} = \frac{\delta^7 Li_{aq,0} - N_{aq} * \delta^7 Li_{aq}}{N_{org}} = \frac{\delta^7 Li_{aq,0} - N_{aq} * \delta^7 Li_{aq}}{(1 - N_{aq})} \tag{12}$$

$$\delta^7 Li_{aq} - \frac{\delta^7 Li_{aq,0} - N_{aq} * \delta^7 Li_{aq}}{(1 - N_{aq})} = 1000(\alpha - 1) \tag{13}$$

Multiplying $(1 - N_{aq})$ with both sides of eq. (13) and rearranging gives:

$$\delta^7 Li_{aq} = 1000(\alpha - 1) * (1 - N_{aq}) + \delta^7 Li_{aq,0} \tag{14}$$

commonly referred to as the batch equation.

The results for the equilibrium conditions (after 30 min in Fig. 2) are plotted in Fig. 4. From linear regression the separation factor is found to be 1.026 ± 0.002, while the correlated intercept (12.163) also agrees well with experimentally measured $\delta^7 Li_{aq,0}$ (12.059).

Studies using similar chemical systems have been summarized in Table 3. These results, including ours, confirm that the system of ionic liquids, diluting solvents, and extractants (B15C5 and its derivatives) are promising candidates for lithium extractive fractionation and will be considered further in the continuous small channel separators.

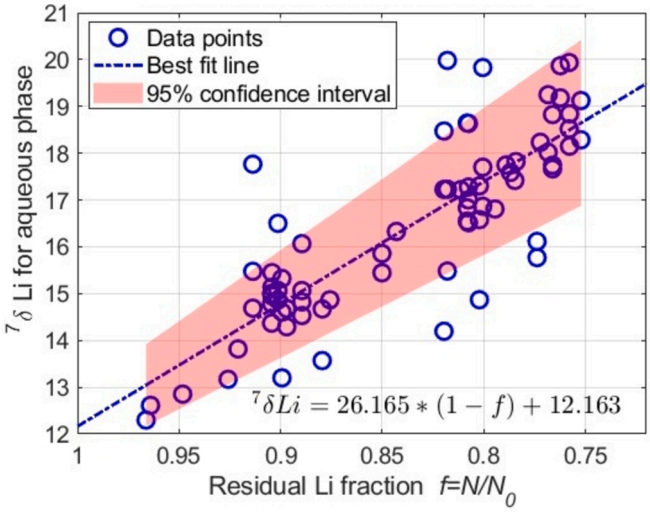

Fig. 4. Li isotope separation factor determined in equilibrium experiments. The residual fraction f is the ratio of remaining lithium in the aqueous solution in molar concentration (N) to that of the overall lithium in the initial aqueous solution (N_0).

Table 3
Summary of extraction results for Li isotope enrichment in experiments in stirred vessels.

Extractant	Solvents	α	Dilution	Safety	Reference
B15C5	Chloroform ($CHCl_3$)	1.017 - 1.044± 0.003	/	toxic	Nishizawa, K., et al., Journal of Nuclear Science and Technology, [22]Shokurova, N.A., et al., Russian Journal of Inorganic Chemistry, [48]Shi, C., et al., Journal of Molecular Liquids, [49]
B15C5	1-(butyl, hexyl, octyl, decyl)-3-methyl-imidazolium-bis (trifluoromethylsulfonyl)imide ([C4,6,8,10 mim]$^+$[NTf2]$^-$)	1.029± 0.001	/	nontoxic	Xiao, J., et al., Journal of Molecular Liquids, [23]
B15C5	1-butyl-3-methylimidazolium hexafluorophosphate ([C4mim][PF6])	1.038± 0.002	Chloroform ($CHCl_3$)	toxic	Xiao, J., et al., Journal of Molecular Liquids, [24]
DB15C5	1-Ethyl-3-methyl-imidazolium-bis (trifluoromethysulfonyl)-imide ([EMIm][NTf2])	1.031 - 1.034± 0.001	Anisole ($CH_3OC_6H_5$)	nontoxic	Sun, H., et al., Fusion Engineering and Design, [32]Zhang Z., et al., Journal of Molecular Liquids, [33]
DB15C5	1-hexyl-3-methylimidazolium bis (trifluormethylsulfonyl)imide ([HMIM][NTf2])	1.037± 0.002	Anisole ($CH_3OC_6H_5$)	nontoxic	Zhang, Z., et al., Fusion Engineering and Design, [50]
B15C5	1–Butyl–3–methylimida–zolium bis (trifluoromethylsulfonyl)imide ([C4mim][NTf2])	1.030± 0.002	Anisole ($CH_3OC_6H_5$)	nontoxic	Liu, B., et al., Journal of Molecular Liquids, [29]
B15C5	1–Butyl–3–methylimida–zolium bis (trifluoromethylsulfonyl)imide ([C4mim][NTf2])	1.026± 0.002	Anisole ($CH_3OC_6H_5$)	nontoxic	Current work

3.2. DFT calculations of fractionation mechanisms

In stirred vessels, equilibrium can be established over long residence times, and the extraction is underpinned by the thermodynamic characteristics. The results in the previous section show that the lithium isotopes fractionate during extraction while there is a one-to-one ratio between the extractant molecule and the lithium ion transferred. Yet the mechanism for lithium extractive separation on a molecular level, as well as the role of the organic phase composition remain unknown. Density Functional Theory (DFT) calculations can provide further insights at atomistic level and help interpret the fractionation results found experimentally. The DFT calculations are used to study the mechanism of lithium isotope fractionation with the extractant B15C5, and to investigate the impact of the organic phase composition on the isotope separation. The detailed models can be found in the Supplementary Material.

As a first step, the configurations of lithium species in both phases are optimised. In the aqueous phase, lithium ions have a hydrated structure which has been verified by many studies [51,52]. The most stable structure is lithium ion coordinated with four water molecules, as shown in Fig. 5(a). In the organic phase, lithium ions are captured by the extractant which has a negative cavity of similar size to the lithium ion, as shown in Fig. 5(b) and (c). Detailed information on the optimisation can be found in the Supplementary Material.

DFT calculations were then performed to analyse the fractionation mechanism by solving for the vibrational frequency of the Li-O bonds in the aqueous and the organic solutions. Hooke's law (equation(15)) shows that the vibrational frequency (ν) of the bond is proportional to the force constant (k).

$$\nu = \frac{1}{2\pi}\sqrt{\frac{k}{m}} \tag{15}$$

where m stands for the reduced mass (defined as the ratio of the product of atomic masses to the sum of atomic masses). According to the

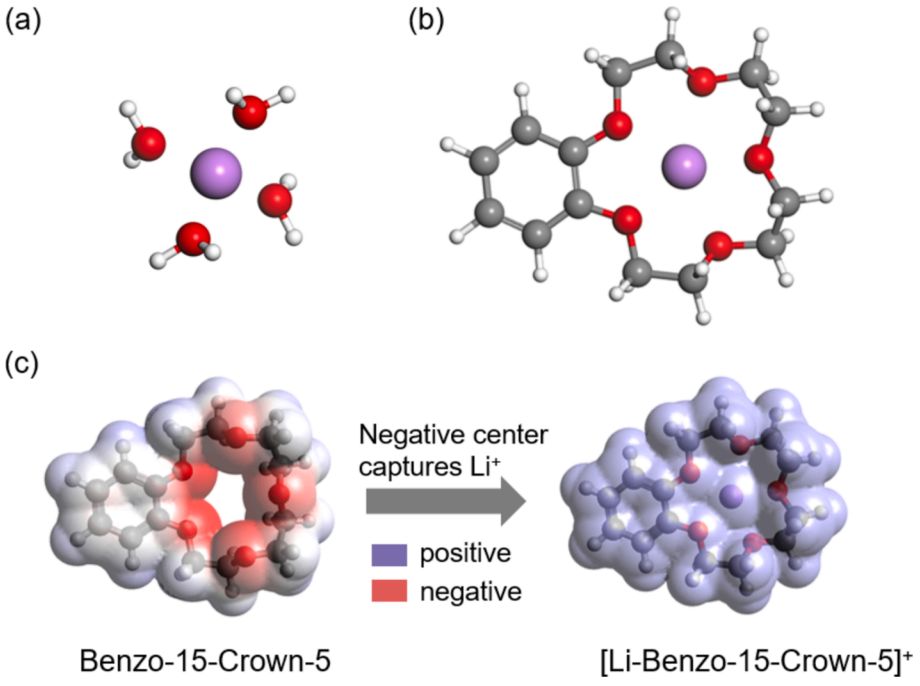

Fig. 5. Optimized structures for (a) $Li(H_2O)_4^+$; (b) $[Li\text{-}B15C5]^+$; (c) electrostatic *iso*-surfaces of $\rho(r) = 0.001e/bohr^3$ for B15C5 and $[Li\text{-}B15C5]^+$. Purple, red, white, and grey spheres denote lithium, oxygen, hydrogen, and carbon atoms, respectively.

quantum mechanical solution for an harmonic oscillator (Eq.(16)), the internuclear potential energy (E_n) is proportional to vibrational frequency (ν) of the bond.

$$E_n = \left(n+\frac{1}{2}\right)h\nu \tag{16}$$

where n stands for the non-negative quantum number (0, 1, 2…) associated with the energy level of the oscillator, and h represents Planck's constant. The vibrational frequencies of the Li-O bonds are calculated and listed in Table 4. Comparing the vibrational frequencies υ_6 and υ_7 for the complex $Li(H_2O)_4^+$, it is found that υ_7 exhibits a smaller value for all the modes that have been considered. Therefore, ^{7}Li-O in the aqueous solution has relatively smaller zero-point energy at the ground state, making the ^{7}Li-O bond more thermodynamically stable. This reduces the likelihood for ^{7}Li to enter the other phase from the aqueous solution compared to ^{6}Li. Table 4 also shows that compared with $Li(B5C15)^+$, the complex $Li(H_2O)_4^+$ has higher Li-O vibrational frequencies, irrespective of the isotope ^{7}Li or ^{6}Li present in the complexes. Consistent with Bigeleisen's findings that the heavier isotope is more stable in a strong bond phase with high vibrational frequency [53], the difference in lithium vibrational frequencies between the two media also confirms that ^{7}Li ions tend to remain in the aqueous phase where the bonds are strong, while ^{6}Li ions are preferentially captured by B15C15 in the organic phase.

The influence of diluting the ionic liquid with anisole was also studied with DFT calculations, by considering the change in permittivity, or dielectric constants of the organic phase. The permittivity of a solvent influences the harmonic structure of the molecules within it and can change the thermodynamic characteristics in isotope exchange reactions. We have determined the structures of 1:1 stoichiometry Li-(B5C15) as discussed above. Experimental studies have revealed the existence of complex $Li(B15C5)(H_2O)^+$ in the organic side, which consists of Li^+ coordinated with the five O atoms from B15C5 and one O atom from H_2O [54]. Meanwhile, a corresponding number of anions must exist in the organic phase for electrical neutrality. It has been reported that for a crown ether/LiX-H2O extraction system, lithium ions can transfer together with their anions into the organic phase forming ion pairs [Li-crown ether-H_2O]$^+X^-$ (X for Cl, Br, or I)[55,56]. In the presence of IL, both chloride and NTf2 (denoted as $CF_3SO_2NSO_2CF_3$) anions should be considered as possible candidates to pair with the lithium-extractant complex. The optimised structures in the two reactions are shown in the supplementary material [55,56]. The isotopic exchange reactions are as follows:

Reaction (1):

$$^6Li(H_2O)_4Cl(aq) + {}^7Li(B15C5)(H_2O)Cl(org) \Leftrightarrow {}^7Li(H_2O)_4Cl(aq) + {}^6Li(B15C5)(H_2O)Cl(org)$$

Reaction (2):

$$^6Li(H_2O)_4Cl(aq) + {}^7Li(B15C5)(H_2O)NTf2(org) \Leftrightarrow {}^7Li(H_2O)_4Cl(aq) + {}^6Li(B15C5)(H_2O)NTf2(org)$$

DFT simulations were performed to determine the thermodynamic parameters at a temperature of 293.15 K and 1 atm and identity the spontaneity of the two isotopic exchange reactions. Table 5 shows the Gibbs free energy change (ΔG), enthalpy change (ΔH), and entropy change (ΔS) for each reaction with different anionic ligands in different solutions. The negative Gibbs free energy change shows both isotopic exchange reactions are spontaneous regardless of the composition of the organic phase. This suggests that lithium-6 in the aqueous phase always tends to exchange with lithium-7 in the organic phase, with or without the participation of the ionic liquid anion. In addition, Reaction (2) has significantly smaller Gibbs free energy, making it more favourable than Reaction (1). It shows that the addition of ionic liquid facilitates the isotope exchange by enabling a more thermodynamically favourable pathway. Comparing the values of ΔG, ΔH, and ΔS for both reactions in Table 5 for different solvation environments (pure ionic liquid and anisole diluted ionic liquid), it is found that the dilution with anisole has no significant impact on the performance of isotopic exchange from the perspective of thermodynamic parameters. The negative values of enthalpy change suggest that the lithium isotope exchange is exothermic reaction, and the negative entropy change indicates that the reaction favours low temperature. These thermodynamic parameters in Table 5 show that the existence of NTf2 anions can enhance the separation of ^{6}Li/^{7}Li isotopes, and IL dilution with anisole plays an insignificant role from a thermodynamic perspective (i.e., at equilibrium state).

3.3. Continuous flow extraction in small channels

The patterns of the organic-aqueous mixtures obtained in the small channel with a T-junction inlet, are annular, churn, drop, intermittent and plug flow and are plotted in the map in Fig. 6. Plug flow occupies a large area of the map for mixture velocities less than 0.01 m/s and is characterised by well-defined dispersed phase plugs, with length larger that the channel diameter, separated by continuous phase slugs. This pattern is characterised by the thin film between the plug and the channel wall, recirculation patterns within the phases as well as large interfacial areas which improve mass transfer within and across the phases [57,58]. For liquid–liquid extractions in a small channels under different flow regimes, it has been found that the volumetric mass transfer coefficient decreases as the flow regime changes from plug flow to annular and plug-annular flow [59]. Also, the pressure drop of annular and plug-annular flows is much larger than that of plug flow, causing a significant increase in operating and pumping costs. Therefore, plug flow has been used for the flow extraction studies reported here.

To investigate the effects of residence time without influencing the flow patterns, the mixture velocity was kept constant at 0.01 m/s while the length of the test channels varied from 15 to 75 cm at intervals of 15 cm. The amount of lithium extracted is given in terms of extraction percentage E_p, defined as by:

$$E_p = \frac{C_{aq,0} - C_{aq,t}}{C_{aq,0}} \times 100\% \tag{17}$$

Table 4
Harmonic vibrational frequencies of Li-O bond at 0 k with isotopic shifts ($\Delta\upsilon$) between ^{6} Li-O (υ_6) and ^{7} Li-O (υ_7) in complexes $Li(H_2O)_4^+$ and $Li(B15C5)^+$, and average Li-O distance (d). The modes refer to specific patterns of atomic motion within a molecule which can be found in supplementary material.

Complex	Modes	υ_6(cm^{-1})	υ_7(cm^{-1})	d (Å)
$Li(H_2O)_4^+$	B1	536	517	1.98
	B2	529	506	
	E	526	503	
$Li(B15C5)^+$	A	396	390	2.19
	B	345	337	

Table 5
DFT calculated the Gibbs free energy change (ΔG), enthalpy change (ΔH), and entropy change (ΔS) for the isotopic exchange reactions at 293.15 K, with thermal correction to enthalpy. Two different solvation environments are considered by using COSMO, with different dielectric constants (C^2 /(N·m^2)$^{-1}$): 11.6 for pure IL and 6.4 for anisole diluted IL.

Environment	Reaction	ΔH(kJ/mol)	ΔS(J/mol/K)	ΔG(kJ/mol)
Pure IL	Reaction1 (Cl)	−0.081	−0.230	−0.014
	Reaction2 (NTf2)	−0.115	−0.280	−0.033
7 Anisole: 3 IL	Reaction1 (Cl)	−0.086	−0.234	−0.017
	Reaction2 (NTf2)	−0.119	−0.285	−0.036

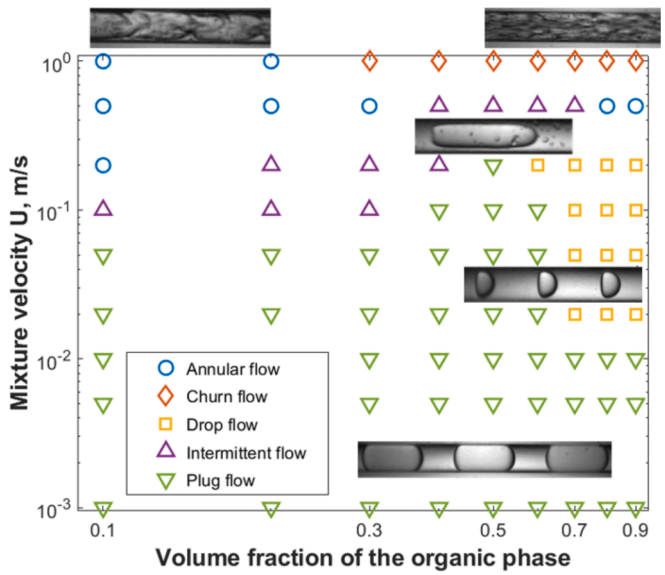

Fig. 6. Flow patterns in the small channel. Mixture velocity is defined as $U = (Q_w + Q_o)/\left[\pi\left(\frac{d}{2}\right)^2\right]$, while volume fraction is defined as $\varphi = Q_o/(Q_w + Q_o)$.

where C_{aq} denotes the lithium concentration in the aqueous phase, and subscripts *0* and *t* represent the initial solution and the solution sampled at residence time *t*, respectively. Extraction efficiency E_e is used to indicate the amount extracted at residence time *t* compared to the equilibrium extracted at equilibrium, and is defined as

$$E_e = \frac{C_{aq,0} - C_{aq,t}}{C_{aq,0} - C_{aq,eq}} \times 100\% \quad (18)$$

The results of E_p and E_e are given in Fig. 7. As it can be seen in Fig. 7(a), for extractant concentration of 0.5 mol/L the extraction percentage has already reached 15 % at residence time of 15 s, regardless of the composition of the organic phase. As a comparison, it takes 10 min to reach ~12.5 % extraction percentage in the batch system (Fig. 2). In the flow channel, the extraction percentage reaches around 19 % within 75 s. For the low extractant concentration (0.2 mol/l), the extraction percentage increases to 8 % at 45 s, while similar extraction percentage is achieved in about 40 min in the batch vessel. From Fig. 7(b) at high extractant concentrations (0.5 mol/L), the extraction efficiency E_e exceeds 60 % within 15 s. As the residence time increases further, there is a gradual increase towards 80 %. When the extractant concentration is low (0.2 mol/L), the extraction efficiency undergoes a sharp increase at the beginning, reaching about 75 % at 45 s, followed by a slight increase afterwards. Comparing with stirred vessels, extractions in small channels can significantly reduce the residence times to achieve the required extraction efficiencies, especially when pure ionic liquids are used (i.e., no anisole dilution). The addition of anisole diluent further reduces the time to reach equilibrium in the reactor (Fig. 2). No significant influence of diluting IL with anisole is observed in terms of extraction percentage or extraction efficiency.

The fractionation factors of lithium isotopes during the flow extraction in channels are plotted in Fig. 8. As it can be seen, the fractionation factor is 1.032 (±0.005), while the intercept is equal to 11.744, which agrees well the experimentally measured $\delta^7 Li_{aq,0}$(12.059). As Fig. 7 suggests, equilibrium has not been reached in the small channels as the data points do not reach 100 % extraction efficiency before 75 s. It seems that for these cases the 'fractionation factor' is larger than the one obtained at equilibrium conditions (1.026 ± 0.002).

Here, a parameter called apparent fractionation factor $\tilde{\alpha}$ is introduced to quantify the ratio of the instantaneous delta lithium-7 values in the two phases, using the definition of Eq. (5). Results for $\tilde{\alpha}$, plotted in

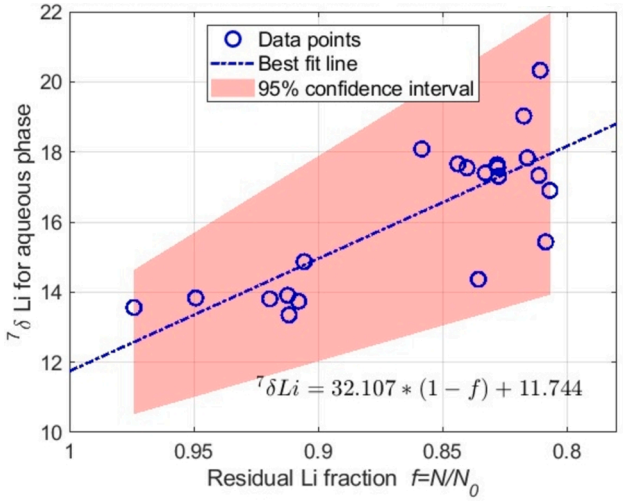

Fig. 8. Li isotope separation factor determined in microfluidic channels.

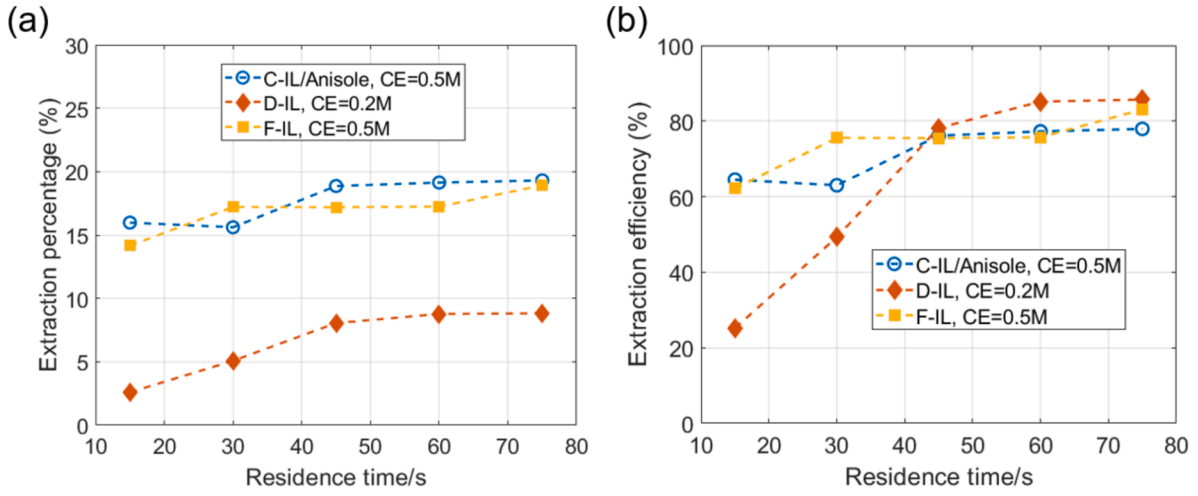

Fig. 7. (a) Extraction percentage of lithium ions in microfluidic channels at different residence times. (b) Extraction efficiency of lithium ions in microfluidic channels at different residence times.

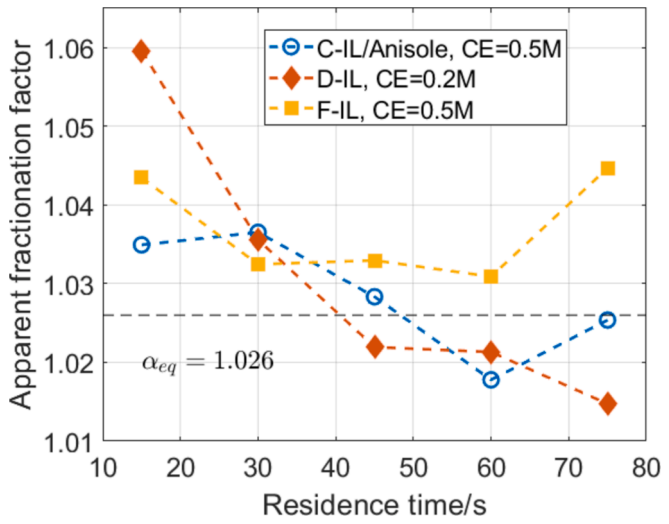

Fig. 9. (a) Apparent fractionation factor $\tilde{\alpha}$ at different residence times t in microfluidic reactors. (b) extraction efficiency over residence times in microfluidic reactors. The dotted horizontal line represents the fractionation factor at equilibrium state.

Fig. 9 against the residence time in the channel, show that in all cases studied the apparent fractionation factor is higher than α at equilibrium for residence times between 15 s and 30 s. As residence time increases, the apparent fractionation factor gradually converges around the equilibrium value. It seems that lithium-6 is transported more rapidly from the aqueous to the organic phase especially at the beginning, yielding $\tilde{\alpha}$ larger than the equilibrium value. These results strongly encourage the consideration of kinetic characteristics for lithium fractionation in small channel contactors. It has been found that the difference in the diffusion coefficients of the isotopes in solids and water depends on the isotope atomic masses and can empirically be described by the following equation:

$$\frac{D_{^6Li}}{D_{^7Li}} = \left(\frac{m_{^7Li}}{m_{^6Li}}\right)^{\beta} \tag{19}$$

where β can be experimentally determined for different media. By measuring the arrested diffusion of lithium, it was documented that lithium-6 diffuses up to 3 % faster than lithium-7 in both silicate melt and in water [60]. In small channels, diffusion is a primary mechanism governing mass transport. This difference in diffusion rates could explain the high apparent fractionation factor at short residence times. By considering the results in both Figs. 7 and 9, a trade-off can be found between the amount of lithium extracted and the degree of lithium enrichment in the flow separators. Larger residence times result in larger amount of lithium extracted into the organic phase, while the degree of fractionation decreases.

4. Conclusions

The study explored the separation of lithium isotopes using liquid–liquid extraction, where the organic phase comprised either ionic liquid (1-butyl-3-methylimidazolium bis (trifluoromethyl sulfonyl) imide ([C4mim][NTf2])) alone or combined with anisole, with benzo-15-crown-5 included as the extractant. Experiments were carried out in stirred vessels and in small channels. Extractant concentrations of 0.1, 0.2, 0.3, 0.4, and 0.5 mol/L were used while the initial LiCl concentrations in the aqueous phase was 0.5 mol/L. In the equilibrium experiments in the stirred vessels, it was found that the extraction percentage increased with extractant concentration, and a maximum of about 23 % lithium in the organic phase was reached for extractant concentration of 0.5 mol/L. Diluting the ionic liquid with anisole did not change the extraction percentage at equilibrium, but it decreased the time required to reach the equilibrium concentration. The fractionation factor was found to be $\alpha = 1.026$ (± 0.002), which agrees well with previous studies for this system and other similar systems in stirred vessels.

Calculations with Density Functional Theory (DFT) suggested that lithium isotopes are fractionated due to different vibrational frequencies of the Li-O bond in crown ether (350 cm^{-1}) and in water (520 cm^{-1}). Both the experimental results and the DFT calculations support the mechanism that the extractant predominantly forms a one-to-one complex with lithium ions in the organic phase during extraction. In addition, it was found that the ionic liquid helps the isotope fractionation by enabling a preferred reaction pathway, while its dilution with anisole does not significantly affect it. The dilution with anisole, however, reduces the viscosity of the diluent and can improve the usage of the ionic liquid.

For the continuous extractions in small flow channels, velocities that resulted in plug flow were chosen (0.01 m/s). The extraction efficiency reached about 80 % within 1 min, which is significantly reduced from the hours required in the stirred vessel experiments. An apparent fractionation factor of 1.032 (± 0.005) was found which is higher than that in stirred vessels, due to enhanced diffusion of the lithium-6 isotope. With an increase in residence time in the small channels, the apparent fractionation factors were found to decrease and converge around the equilibrium values. This suggests that small channels could enhance lithium-6 enrichment compared to stirred vessel separators by taking advantage of differences in the diffusion rate of the isotopes.

The results show that the separation of lithium by solvent extraction in small channels is significantly faster than in batch systems. In addition, the apparent fractionation of the lithium isotopes at very short times in the small channels is larger than the equilibrium one, which is advantageous for enrichment. Further studies can explore the trade-off between the extraction percentage and the fractionation of the isotopes as well as the scale up of the small channel contactors. The conditions for the extraction and fractionation, such as temperature, lithium salt concentration, and pH value should be further explored in future work.

CRediT authorship contribution statement

Cong Duan: Methodology, Formal analysis, Investigation, Writing – original draft. **Shijia Sun:** Writing – original draft. **Haoyu Wang:** Conceptualization, Validation, Investigation. **Mohd Tarique:** Investigation. **Edward Tipper:** Resources, Investigation, Methodology. **Tamsin Whitfield:** Conceptualization, Supervision, Writing – review & editing. **Mark R. Gilbert:** Conceptualization, Funding acquisition, Supervision, Writing – review & editing. **Panagiota Angeli:** Conceptualization, Funding acquisition, Supervision, Project administration, Writing – review & editing.

Declaration of competing interest

The authors declare that they have no known competing financial interests or personal relationships that could have appeared to influence the work reported in this paper.

Acknowledgements

Cong Duan would like to acknowledge the financial support from UCL and the China Scholarship Council. This work has been part-funded by the EPSRC Energy Programme [grant number EP/W006839/1]. The authors acknowledge the use of the UCL Kathleen High Performance Computing Facility (Kathleen@UCL) and associated support services, in the completion of this work.

Appendix A. Supplementary data

Supplementary data to this article can be found online at https://doi.org/10.1016/j.seppur.2025.131525.

Data availability

Data will be made available on request.

References

[1] R.S. Hindshaw, S.M. Aciego, E.T. Tipper, Li and U isotopes as a potential tool for monitoring active layer deepening in permafrost dominated catchments, Front. Earth Sci. 6 (2018), https://doi.org/10.3389/feart.2018.00102.

[2] T.I. Taylor, H.C. Urey, Fractionation of the lithium and potassium isotopes by chemical exchange with zeolites, J. Chem. Phys. 6 (8) (1938) 429–438, https://doi.org/10.1063/1.1750288.

[3] G.N. Lewis, R.T. Macdonald, The separation of lithium isotopes, J. Am. Chem. Soc. 58 (12) (1936) 2519–2524, https://doi.org/10.1021/ja01303a045.

[4] J. Liu, Q. Liu, Q. Meng, D. Zhu, X. Liang, The distribution of lithium in nature and the application of lithium isotope tracing, IOP Conf. Ser.: Earth Environ. Sci 600 (1) (2020) 012018, https://doi.org/10.1088/1755-1315/600/1/012018.

[5] T. Giegerich, K. Battes, J.C. Schwenzer, C. Day, Development of a viable route for lithium-6 supply of DEMO and future fusion power plants, Fusion Eng. Des. 149 (2019) 111339, https://doi.org/10.1016/j.fusengdes.2019.111339.

[6] M. Ragheb, Isotopic separation and enrichment, Nuclear, plasma and radiation science. Inventing the future. <https://www. researchgate. net/publication/242126786_ISOTOPIC_SEPARATION_AND_ENRICHMENT>. Accessed 15 (2015).

[7] M. Fujie, Y. Fujii, M. Nomura, M. Okamoto, Isotope effects in electrolytic formation of lithium amalgam, J. Nucl. Sci. Technol. 23 (4) (1986) 330–337, https://doi.org/10.1080/18811248.1986.9734990.

[8] E.A. Symons, Lithium isotope separation: a review of possible techniques, Sep. Sci. Technol. 20 (9–10) (1985) 633–651, https://doi.org/10.1080/01496398508060696.

[9] Y. Ban, M. Nomura, Y. Fujii, Chromatographic separation of lithium isotopes with silica based Monobenzo-15-crown-5 resin, J. Nucl. Sci. Technol. 39 (3) (2002) 279–281, https://doi.org/10.1080/18811248.2002.9715187.

[10] J.R. Black, G. Umeda, B. Dunn, W.F. McDonough, A. Kavner, Electrochemical isotope effect and lithium isotope separation, J. Am. Chem. Soc. 131 (29) (2009) 9904–9905, https://doi.org/10.1021/ja903926x.

[11] T. Hoshino, T. Terai, High-efficiency technology for lithium isotope separation using an ionic-liquid impregnated organic membrane, Fusion Eng. Des. 86 (9) (2011) 2168–2171, https://doi.org/10.1016/j.fusengdes.2011.03.090.

[12] T. Arisawa, Y. Maruyama, Y. Suzuki, K. Shiba, Lithium isotope separation by laser, Appl. Phys. B 28 (1) (1982) 73–76, https://doi.org/10.1007/BF00693895.

[13] S.-L. Badea, V.-C. Niculescu, A.-M. Iordache, New trends in separation techniques of lithium isotopes: a review of chemical separation methods, Materials 16 (10) (2023) 3817.

[14] Y. Sun, Q. Wang, Y. Wang, R. Yun, X. Xiang, Recent advances in magnesium/lithium separation and lithium extraction technologies from salt lake brine, Sep. Purif. Technol. 256 (2021) 117807, https://doi.org/10.1016/j.seppur.2020.117807.

[15] B.E. Jepson, G.A. Cairns, Lithium isotope effects in chemical exchange with (2,2,1) cryptand United States, 1979, 16.

[16] K. Nishizawa, H. Watanabe, S.-I. Ishino, M. Shinagawa, Lithium isotope separation by cryptand (2B, 2, 1) polymer, J. Nucl. Sci. Technol. 21 (2) (1984) 133–138, https://doi.org/10.1080/18811248.1984.9731024.

[17] L. Cui, S. Li, J. Kang, C. Yin, Y. Guo, H. He, F. Cheng, A novel ion-pair strategy for efficient separation of lithium isotopes using crown ethers, Sep. Purif. Technol. 274 (2021) 118989, https://doi.org/10.1016/j.seppur.2021.118989.

[18] L. Mao, P. Zhang, H. Ju, X. Zhou, Z. Xue, C. Wang, J. Sun, Y. Jia, F. Shao, X. Zou, B. Li, Y. Jing, Solvent extraction for lithium isotope separation by 4-NO2-B15C5/[BMIm][NTf2] system, J. Mol. Liq. 367 (2022) 120357, https://doi.org/10.1016/j.molliq.2022.120357.

[19] T. Ault, K. Brozek, L. Fan, M. Folsom, J. Kim, J. Zeismer, Lithium isotope enrichment: feasible domestic enrichment alternatives, Dep. Nucl. Eng. Univ. Calif. (2012).

[20] T. Nakano-Ohta, T. Kubota, A. Ando, T. Fujii, S. Fukutani, E. Nakata, T. Nakano, Y. Mahara, Isotopic investigations for the origin of relic from the Matsusaki site Japan, Appl. Radiat. Isot. 67 (7) (2009) 1479–1483, https://doi.org/10.1016/j.apradiso.2009.02.047.

[21] S. Kitazawa, K. Kimura, H. Yano, T. Shono, Lipophilic crown-4 derivatives as lithium ionophores, J. Am. Chem. Soc. 106 (23) (1984) 6978–6983, https://doi.org/10.1021/ja00335a019.

[22] K. Nishizawa, S.-I. Ishino, H. Watanabe, M. Shinagawa, Lithium isotope separation by liquid-liquid extraction using benzo-15-crown-5, J. Nucl. Sci. Technol. 21 (9) (1984) 694–701, https://doi.org/10.1080/18811248.1984.9731102.

[23] J. Xiao, Y. Jia, C. Shi, X. Wang, S. Wang, Y. Yao, Y. Jing, Lithium isotopes separation by using benzo-15-crown-5 in eco-friendly extraction system, J. Mol. Liq. 241 (2017) 946–951.

[24] J. Xiao, Y. Jia, C. Shi, X. Wang, Y. Yao, Y. Jing, Liquid-liquid extraction separation of lithium isotopes by using room-temperature ionic liquids-chloroform mixed solvent system contained benzo-15-crown-5, J. Mol. Liq. 223 (2016) 1032–1038.

[25] M. Davoudi, M.H. Mallah, Enrichment of 6Li using dispersive liquid–liquid microextraction as a highly efficient technique, Ann. Nucl. Energy 62 (2013) 499–503, https://doi.org/10.1016/j.anucene.2013.07.010.

[26] K. Nishizawa, T. Takano, I. Ikeda, M. Okahara, Extractive separation of lithium isotopes by crown ethers, Sep. Sci. Technol. 23 (4–5) (1988) 333–345.

[27] M. Atanassova, Solvent extraction chemistry in ionic liquids: an overview of f-ions, J. Mol. Liq. 343 (2021) 117530, https://doi.org/10.1016/j.molliq.2021.117530.

[28] C. Shi, Y. Jia, J. Xiao, X. Wang, Y. Yao, Y. Jing, Lithium isotope separation by liquid-liquid extraction using ionic liquid system containing dibenzo-14-crown-4, J. Mol. Liq. 224 (2016) 662–667, https://doi.org/10.1016/j.molliq.2016.10.081.

[29] B. Liu, S. Wang, Y. Jia, W. Zhu, Q. Zhang, X. Wang, Y. Yao, Y. Jing, Lithium isotope separation by crown ethers of different nitrogen-containing derivatives in the ionic liquid-anisole system, J. Mol. Liq. 272 (2018) 548–553.

[30] P. Zhang, C. Wang, Z. Xue, L. Mao, J. Sun, F. Shao, M. Qi, Y. Jing, Y. Jia, Extraction separation of lithium isotopes with Bromobenzene-15-crown-5/ionic liquids system: experimental and theoretical study, J. Mol. Liq. 364 (2022) 120020, https://doi.org/10.1016/j.molliq.2022.120020.

[31] L. Cui, R. Gao, Q. Zhang, K. Jiang, H. He, W.-L. Ding, F. Cheng, Benzo-15-crown-5 functionalized ionic liquids with enhanced stability for effective separation of lithium isotopes: the effect of alkyl chain length, ACS Sustain. Chem. Eng. 12 (3) (2024) 1221–1232, https://doi.org/10.1021/acssuschemeng.3c05171.

[32] H. Sun, Y. Jia, B. Liu, Y. Jing, Q. Zhang, F. Shao, Y. Yao, Separation of lithium isotopes by using solvent extraction system of crown ether-ionic liquid, Fusion Eng. Des. 149 (2019) 111338.

[33] Z. Zhang, Y. Jia, B. Liu, H. Sun, Y. Jing, Q. Zhang, F. Shao, M. Qi, Y. Yao, Study on behavior of lithium ion in solvent extraction and isotope separation, J. Mol. Liq. 324 (2021) 114709.

[34] Y.-V. Phakoukaki, P. O'Shaughnessy, P. Angeli, Intensified liquid-liquid extraction of biomolecules using ionic liquids in small channels, Sep. Purif. Technol. 282 (2022) 120063, https://doi.org/10.1016/j.seppur.2021.120063.

[35] H. Wang, P. Angeli, Intensified solvent extraction of L-tryptophan in small channels using D2EHPA, Chem. Eng. Process. - Process Intesif. 172 (2022) 108802, https://doi.org/10.1016/j.cep.2022.108802.

[36] C. Pheasey, P. Angeli, Intensified Nd extraction in small channels for NdFeB magnet recycling, Sep. Purif. Technol. 311 (2023) 122958, https://doi.org/10.1016/j.seppur.2022.122958.

[37] D. Tsaoulidis, E.G. Ortega, P. Angeli, Intensified extraction of uranium(VI) in impinging-jets contactors, Chem. Eng. J. 342 (2018) 251–259, https://doi.org/10.1016/j.cej.2018.02.049.

[38] Y. He, T. Zhang, L. Lv, W. Tang, Y. Wang, S. Tang, Intensifying the extraction of rare earth elements by a mini-channel counter-current extractor, Sep. Purif. Technol. 333 (2024) 125930, https://doi.org/10.1016/j.seppur.2023.125930.

[39] Q. Li, P. Angeli, Intensified Eu(III) extraction using ionic liquids in small channels, Chem. Eng. Sci. 143 (2016) 276–286, https://doi.org/10.1016/j.ces.2016.01.004.

[40] D. Tsaoulidis, M. Mamtora, M.M. Gañet, E. Garciadiego-Ortega, P. Angeli, Scale-up studies for Co/Ni separations in intensified reactors, Micromachines 11 (12) (2020) 1106.

[41] B. Liu, Y. Jia, Z. Zhang, H. Sun, Y. Yao, Y. Jing, M. Qi, Q. Zhang, Separation of lithium isotopes by crown ether-room temperature ionic liquid-anisole friendly solvent system, J. Mol. Liq. 340 (2021) 117207, https://doi.org/10.1016/j.molliq.2021.117207.

[42] J. Tian, Q. Tang, Y. Zhang, Y. Shu, L. Zhang, W. Zheng, A study on the viscosity, density, and derivative properties of 1-alkyl-3-methylimidazolium bis((trifluoromethyl)sulfonyl)imides with benzo-15-crown-5 binary mixtures, J. Chem. Res. 47 (1) (2023) 17475198231156358, https://doi.org/10.1177/17475198231156358.

[43] P. Zhang, Z. Xue, C. Wang, J. Sun, F. Shao, X. Zou, B. Li, M. Qi, Y. Jing, Y. Jia, Mechanisms of ionic liquids on the enhancement of interfacial transport of lithium ions in crown ether system, J. Clean. Prod. 366 (2022) 132782, https://doi.org/10.1016/j.jclepro.2022.132782.

[44] R. Millot, N. Vigier, J. Gaillardet, Behaviour of lithium and its isotopes during weathering in the Mackenzie Basin Canada, Geochim. Cosmochim. Acta 74 (14) (2010) 3897–3912, https://doi.org/10.1016/j.gca.2010.04.025.

[45] J. Carignan, N. Vigier, R. Millot, Three secondary reference materials for lithium isotope measurements: Li7-N, Li6-N and LiCl-N solutions, Geostand. Geoanal. Res. 31 (1) (2007) 7–12, https://doi.org/10.1111/j.1751-908X.2007.00833.x.

[46] J.R. O'Neil, Theoretical and experimental aspects of isotopic fractionation, Rev. Mineral. 16 (1986) 1–40.

[47] A. Rybinska-Fryca, A. Sosnowska, T. Puzyn, Prediction of dielectric constant of ionic liquids, J. Mol. Liq. 260 (2018) 57–64.

[48] N. Shokurova, L. Demina, V. Zhilov, S. Demin, A.Y. Tsivadze, Study of isotope effect upon lithium iodide complexation with benzo-15-crown-5 in water–chloroform extraction system, Russ. J. Inorg. Chem. 61 (2016) 787–790.

[49] C. Shi, Y. Jing, Y. Jia, Solvent extraction of lithium ions by tri-n-butyl phosphate using a room temperature ionic liquid, J. Mol. Liq. 215 (2016) 640–646.

[50] Z. Zhang, Y. Jia, B. Liu, H. Sun, Y. Jing, Q. Zhang, F. Shao, M. Qi, Y. Yao, Extraction and separation of lithium isotopes by using organic liquid film extraction system of crown ether-ionic liquid, Fusion Eng. Des. 161 (2020) 112015.

[51] S.B. Rempe, L.R. Pratt, G. Hummer, J.D. Kress, R.L. Martin, A. Redondo, The hydration number of Li+ in liquid water, J. Am. Chem. Soc. 122 (5) (2000) 966–967, https://doi.org/10.1021/ja9924750.

[52] K. Yamaji, Y. Makita, H. Watanabe, A. Sonoda, H. Kanoh, T. Hirotsu, K. Ooi, Theoretical estimation of lithium isotopic reduced partition function ratio for lithium ions in aqueous solution, Chem. A Eur. J. 105 (3) (2001) 602–613, https://doi.org/10.1021/jp001303i.

[53] J. Bigeleisen, M.G. Mayer, Calculation of equilibrium constants for isotopic exchange reactions, Technical Information Division Oak Ridge Operations, 1947.
[54] B. Yan, P.N. Horton, A.E. Russell, C.J. Wedge, S.C. Weston, M.C. Grossel, Crown ether alkali metal TCNQ complexes revisited – the impact of smaller cation complexes on their solid-state architecture and properties, CrstEngComm 21 (21) (2019) 3273–3279, https://doi.org/10.1039/C9CE00234K.
[55] L. Cui, X. Yang, J. Wang, H. He, Y. Guo, F. Cheng, S. Zhang, Theoretical prediction of 6Li/7Li separation in solvent extraction system using Urey model, Chem. Eng. J. 358 (2019) 435–445, https://doi.org/10.1016/j.cej.2018.09.181.
[56] R. Boulatov, B. Du, E.A. Meyers, S.G. Shore, Two novel lithium−15-crown-5 complexes: an extended LiCl chain stabilized by crown ether and a dimeric complex stabilized by hydrogen bonding with water, Inorg. Chem. 38 (20) (1999) 4554–4558, https://doi.org/10.1021/ic9904790.
[57] Q. Li, P. Angeli, Experimental and numerical hydrodynamic studies of ionic liquid-aqueous plug flow in small channels, Chem. Eng. J. 328 (2017) 717–736.
[58] C. Yao, Y. Zhao, H. Ma, Y. Liu, Q. Zhao, G. Chen, Two-phase flow and mass transfer in microchannels: a review from local mechanism to global models, Chem. Eng. Sci. 229 (2021) 116017.
[59] A. Matsuoka, K. Mae, Design strategy of a microchannel device for liquid–liquid extraction based on the relationship between mass transfer rate and two-phase flow pattern, Chem. Eng. Process. Process Intensifi. 160 (2021) 108297.
[60] S. Penniston-Dorland, X.-M. Liu, R.L. Rudnick, Lithium isotope geochemistry, Rev. Mineral. Geochem. 82 (1) (2017) 165–217, https://doi.org/10.2138/rmg.2017.82.6.